J Solid State Electrochem (2010) 14:83–91
DOI 10.1007/s10008-009-0789-2

ORIGINAL PAPER

The influence of the surface preparation on the electrodeposition of gold particles on silicon

K. De Henau · I. Huygens · K. Strubbe

Received: 14 October 2008 / Revised: 8 January 2009 / Accepted: 10 January 2009 / Published online: 29 January 2009
© Springer-Verlag 2009

Abstract In a systematical study of the electrodeposition of gold (I) on silicon (100), the influence of the surface preparation on the nucleation behavior of gold was investigated. A two-phase experimental design was used. In the first phase, it was investigated whether there is an influence; in the second phase, an optimization was performed. It was found that more homogeneous particle coverages and higher particle densities can be obtained when the surface is dipped in an acid fluoride solution with small nitric acid to hydrogen fluoride proportions. Furthermore, the observations indicated that more negative deposition potentials also lead to better coverages, higher densities, and less clustering.

Keywords Electrochemical deposition · Gold · Silicon · Surface preparation

Introduction

Gold nanostructures on a silicon surface are known catalysts for the growth of silicon nanowires in the vapor–liquid–solid growth method [1–4]. In order to grow well-defined nanowires, the metal catalysts must all have the same dimensions, because these determine the diameter of the nanowires [5]. Secondly, they have to be distributed homogeneously on the surface, and a large coverage (10^{10} to 10^{12} particles per cm^2) is aimed at in order to insure an optimal yield.

K. De Henau · I. Huygens · K. Strubbe (✉)
Department of Inorganic and Physical Chemistry,
Ghent University,
Krijgslaan 281-S12,
9000 Ghent, Belgium
e-mail: Katrien.Strubbe@UGent.be

A semiconductor surface covered with metal nanoparticles can be obtained in several ways. In one method, the metal is evaporated onto the surface by molecular beam epitaxy, a technique which requires ultrahigh vacuum [6]. Another possibility is to form the particles in solution after which they are deposited on the semiconductor surface. These particles can be synthesized by means of colloid chemistry [7] or laser ablation [8]. Another possible technique, which does not require a vacuum environment, high temperatures, or organic solvents, is electrochemical deposition: nanoparticles can be formed by reduction of metal ions at the interface of the electrode surface and the electrolyte solution when a suitable potential is applied [9].

An important parameter in the electrochemical formation of nanoparticles is the condition of the surface upon which they are deposited. According to nucleation theory, after electron transfer from the electrode to the metal ion in solution, the metal atom will diffuse over the electrode surface until it clusters together with other metal atoms [10] to form a thermodynamic stable cluster. Formation of clusters occurs preferentially at sites where the cluster can coordinate to the surface, such as steps and kinks. A study by Munford et al. [11] about the electrodeposition of gold on silicon (111) showed that nuclei were formed preferentially at steps rather than on the flat surface. The structure of the substrate surface will hence be important for the surface coverage after the deposition.

A commonly used final preparation step of a silicon substrate consists of a dip in a hydrogen fluoride solution, in order to remove oxides and contaminants from the surface and to create a stable hydrogen-terminated surface [12]. Depending on the crystallographic orientation of the surface, different types of hydrides will be present. The ideal termination of a Si(111) surface is a monohydride coverage. The more reactive Si(100) surface will ideally

have a dihydride termination. A real surface shows a lot of imperfections at the atomic scale, and other types of hydrides will be present. Several studies have shown that the nature of the termination and hence the roughness can be controlled by the composition of the hydrofluoric acid (HF) solution [12, 13]. A Si(111) surface, etched in HF at pH 0, is microscopically rough (mono-, di-, and trihydrides are present). By increasing the pH with NH_4OH, the presence of monohydrides increases. At pH 9, an ideal monohydride-terminated silicon surface is obtained. For the more reactive Si(100) surface, the situation is reversed. At low pH values, there will be mainly dihydrides present, which is the ideal termination of an Si(100) surface. A flat, solely dihydride-terminated silicon surface is impossible to obtain though, because such a surface would suffer a great sterical strain. For this reason, an appreciable amount of mono- and trihydrides are also present. Analogous to the Si (111) surface, there will be more and more monohydrides when the pH is increased. It was shown that this is due to the formation of microscopic (111) facets [13].

After HF treatment, the silicon surface is not only H-terminated but also a certain amount of fluoride termination occurs. The relative quantity of this F-termination remains a point of discussion, but there seems to be a consensus concerning following trends [12, 14, 15]:

- The amount of F-termination increases with increasing F-concentration
- The more reactive the silicon surface, the higher the F-termination

When the surface is rinsed with water or alcohol, the fluoride termination will be replaced with hydroxy-, respectively, alkoxy-termination [12]. Another etchant which is often used as a final preparation step for silicon is a HNO_3/HF mixture. The nitric acid oxidizes the surface, whereas the hydrofluoric acid etches this oxide simultaneously. When the native oxide layer is removed, the surface will still be oxidized by this mixture. When the ratio c_{HNO3}/c_{HF} is low, the oxidation step is rate limiting. When on the other hand the ratio c_{HNO3}/c_{HF} is high, the dissolution step determines the etch rate [16]. Due to the high reactivity of the nitric acid, this etching will occur isotropic; all crystal planes will be attacked at equal speed.

It has been shown that the etch rate is the highest in a HNO_3/HF mixture with ratio 4,5 (70% HNO_3)/1 (49% HF) [17]. Addition of NH_3 to this mixture slows the reactions slightly [18].

To our knowledge, a systematic study of the influence of the preparation steps on the electrochemical nucleation behavior of metals upon silicon has not been performed until now. Therefore, we have studied the nucleation behavior of gold on silicon (100) as a function of the composition of the etch solution. We used an experimental design in order to detect the influence of the various factors and possible interactions.

Experimental

Gold nanoparticles were electrodeposited on *n*-type Si (100) substrates (IMEC; Leuven, Belgium). The wafers were backside implanted and had a dotation of approximately 10^{15} cm^{-3}. They were cut into 2×2-cm platelets and incorporated as the electrode in an electrochemical cell. The surface area which was in contact with the solution was 1.76 cm^2. Prior to the fluoride treatment, they were cleaned according to the following steps: a 10-min dip in a (25%) NH_3/(30%) H_2O_2/H_2O (1:1:8) solution, rinse with water, a dip for 10 min in a (95%) H_2SO_4/(30%) H_2O_2/H_2O (1:1:8) mixture followed by a rinse with water. Immediately after this treatment and before every electrochemical experiment, the silicon electrode was etched for 10 min in a fluoride solution of variable composition, containing Suprapur® 40% HF, analytical grade (25%) ammonia to alter pH, and analytical grade (69%) HNO_3 in some solutions. After this etch, the substrates were rinsed with water or an alcohol. In every step and for each solution, double distilled water was used.

Experiments were performed in a three electrode cell with a platinum grid counter electrode and an Ag/AgCl reference electrode. The cell was connected to a potentiostat/galvanostat model 263 A EG&G PAR. In the chronoamperometric experiments, the potential was varied in one step from the open circuit potential (OCP) to a more negative deposition potential V_d, where gold reduction occurs. The electrolyte solution consisted of 5 mM KAu $(CN)_2$, 1 M KOH and 1 M KCN and was N_2 bubbled for at least 20 min prior to the electrochemical experiments. After being corrected for the capacitive current density to strictly Faraday current density j_F, the transients were analyzed by a model for 3D nucleation [19–22]. After electrodeposition, the silicon surface was investigated ex situ by scanning electron microscopy (SEM) and analyzed in ImageJ. The homogeneity of the surface was determined by the relative standard deviation of the mean particle density determined by 64 different areas of 0.27 μm^2 on the surface. Ellipsometric measurements were performed on a Woollam M2000.

In a first series of experiments, the influence of surface preparation on the nucleation process was studied by a 2^{5-1} fractional factorial design. This experimental setup allowed to determine linear main effects and interactions of effects. The conclusions of this experimental design led to the second series of experiments, a circumscribed central composite (CCC) design, in which main effects, quadratic effects, and interactions were determined [23].

Results and discussion

Cyclic voltammetry

The system of gold(I) reduction from a cyanide solution at a silicon electrode has already been extensively studied [9, 24, 25]. It was established that the reaction is a conduction band process and an overpotential is required for the formation of the new gold phase on the silicon surface. In the alkaline gold cyanide solution, no gold(I) reduction occurs at the OCP, which allows to control the process by means of potential. j, V curves with different scan rates are shown in Fig. 1. The peaks in the negative potential region correspond with gold reduction; the hydrogen reduction branches appear at the most negative potentials. For the experiments, the deposition potential windows were chosen based upon the position of the reduction peaks. In the context of this manuscript, it is important to notice that the pretreatment conditions in the referred studies [9, 24, 25] were different from ours: while the group of Oskam used a 10-s dip in 48% HF, we pretreated the silicon surface with a 5-min dip in 2% HF. Since for both sets of experiments the same conclusions were obtained, the current–voltage behavior as a function of pretreatment conditions was not further investigated.

The 2^{5-1} fractional factorial design approach

In this first setup, we wanted to determine which factors have an influence on the nucleation process. The factors that were considered and their levels are listed in Table 1.

The first three factors are related to the composition of the etching solution; the fourth is the rinse after the HF dip and prior to the electrochemical deposition. In all experiments, the potential was held at V_d for 5 s. A total of 16 different experiments with combinations of factor levels −1 and 1 and 2 experiments at factor level 0 were performed. The latter ones allowed determination of statistical significance of the results.

Table 1 Values for the factors at each factor level in the 2^{5-1} fractional factorial design

F	L		
	−1	0	+1
pH	2	7	10
c_{HF} (M)	0.05	2.5	5
c_{HNO3}/c_{HF}	0	2.25	4.5
rinse	Water	Ethanol/water (1:1)	Ethanol
V_d (V vs. Ag/AgCl)	−1.45	−1.5	−1.55

F factors, *L* level

It was possible to classify the results in four major groups. Typical transients for each group are represented in Fig. 2. V_d was always −1.45 V and the substrates were rinsed with water for each of the illustrated measurements.

In the first group, all the transients show a sharp peak which indicates a diffusion limited reduction (Fig. 2, transient 1). The transients were corrected for either the instantaneous or the progressive induction time t_0 and normalized to the peak maxima (j_m, t_m) [26]. These curves were then compared with the theoretical curves for instantaneous and progressive nucleation. Typical normalized transients can be found in Fig. 3. The corresponding SEM image of the surface can be found in Fig. 4a. From Fig. 3, it follows that the deposition occurs according to a mixed progressive/instantaneous nucleation. Particle densities were determined by analysis of the images in ImageJ. It

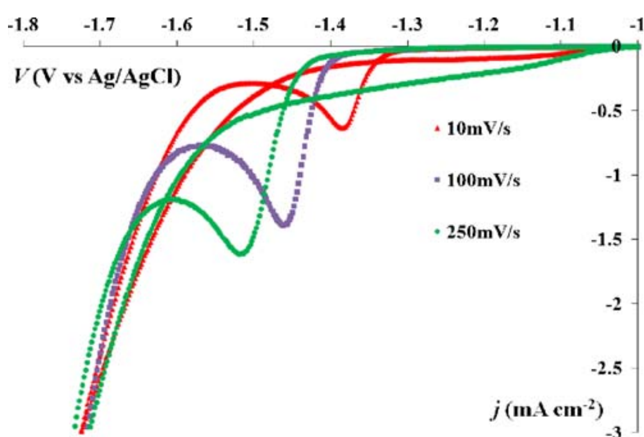

Fig. 1 Current–potential curves for *n*-Si(100) in 5 mM $KAu(CN)_2$+ 1 M KOH+1 M KCN. The scan rate is indicated for each curve in the figure

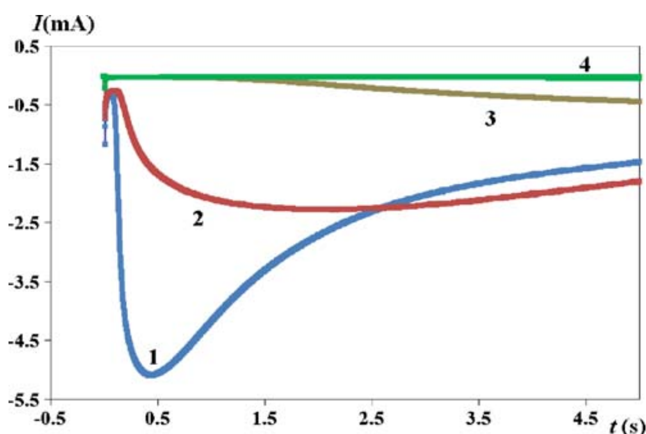

Fig. 2 Typical transients recorded at Si(100) in 5 mM $KAu(CN)_2$+ 1 M KOH+1 M KCN with V_d −1.45 V vs. Ag/AgCl; the substrates were rinsed with water prior to the experiment. The substrates had a different fluoride treatment: *1* pH 2+5 M HF+c_{HNO3}/c_{HF} 4.5; *2* pH 10 +5 M HF+c_{HNO3}/c_{HF} 0; *3* pH 10+0.05 M HF+c_{HNO3}/c_{HF} 0; *4* pH 10 +5 M HF+c_{HNO3}/c_{HF} 4.5

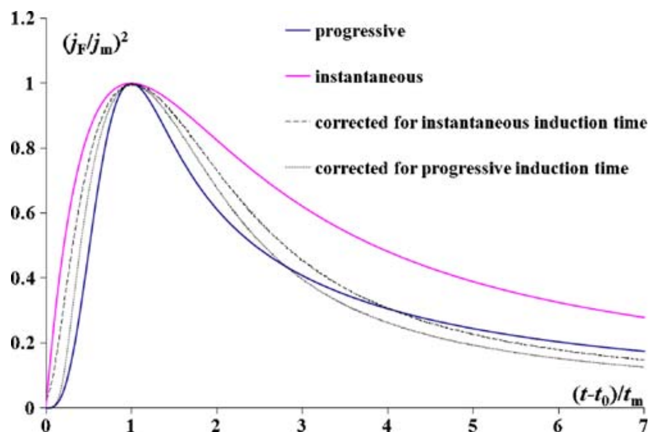

Fig. 3 Group 1 (transients with shape 1 in Fig. 2): dimensionless, corrected transient, recorded at *n*-Si at −1.45 V vs. Ag/AgCl in a solution of 1 M KOH+1 M KCN+5 mM $KAu(CN)_2$. Theoretical curves for instantaneous and progressive nucleation are also shown

appeared that the density had a value in the order of 10^{10} cm^{-2} for all experiments within group 1. The common feature of all these experiments is that the fluoride solution always had a low pH value (factor level −1). Only in this group the substrates were hydrophobic after the HF dip.

The transients in the second group had a different appearance (Fig. 2, transient 2). No sharp peak was seen, but instead the maximum was spread over a large time interval. No significant decrease in current was observed during the time of the measurements. These transients were not only analyzed according to the model of 3D nucleation as mentioned in the "Experimental" section, but also 2D nucleation was considered [27]. None of these models described the nucleation process of the experiments in this group though. The SEM images (Fig. 4b) showed that after deposition, the substrates in this group had a lower particle density (±10^9 cm^{-2}) compared to group 1 (Fig. 4a). All the surfaces in group 2 were treated either with a fluoride solution of neutral pH, or with a solution of high pH with no HNO_3 added. The fluoride concentration was always at least 2.5 M.

In the third group (Fig. 2, transient 3), the *I*, *t* curves showed only a limited current, making it unable to analyze it as transient. Even less particles (±10^8 cm^{-2}) than in the previous groups were present on the surface (Fig. 4c; notice the scale difference with Fig. 4a, b). The common feature of the experiments in this group is that these substrates were dipped in a fluoride solution with high pH, low fluoride concentration, and no HNO_3 added.

The fourth group finally consists of measurements were only a capacitive current was observed. No particles were found on the surface. The fluoride solution was alkaline and HNO_3 was added.

The values for homogeneity were determined for all experiments (see "Experimental" section) and were inserted into the linear model with interactions of the fractional factorial design. These values followed an acceptable normal distribution. Regression showed that there are true effects. A regression coefficient of 0.82 was obtained, which means that the model does not describe the process very well. This might be due to the presence of quadratic or other effects. On the 95% confidence level, two main effects and two interaction terms were significant. Optimization shows that the main effects pH and c_{HNO3} should be low (factor level −1). The interaction terms consist of c_{HF} with either pH or c_{HNO3} in which a high c_{HF} gives a better value for homogeneity. The rinse solvent and deposition potential appear not to be important within the chosen range of values.

The particle densities, *N*, corresponding to the various experiments, were also inserted into the model. Also here, a normal distribution of the values was found and regression showed we are dealing with true effects. The regression coefficient was remarkably better for these results, i.e., 0.98. A complex equation was found on the 95% confidence level. Three main effects (pH, c_{HNO3}, and V_d)

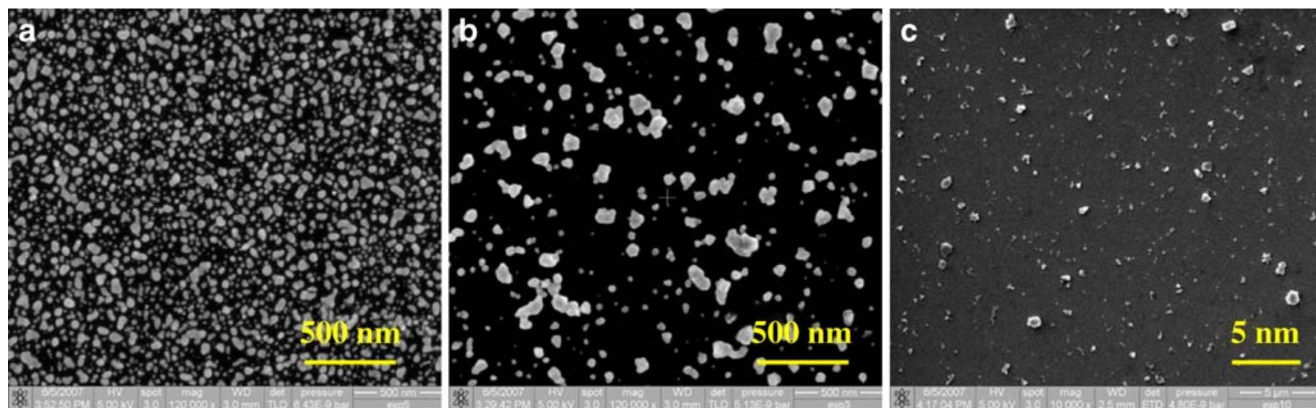

Fig. 4 **a** Typical SEM image of group 1; **b** typical SEM image of group 2; **c** typical SEM image of group 3

and six interactions in which all factors are concerned were determined. Optimization according to this equation consists of using solutions with low pH, low amounts of HNO_3, high concentrations of fluoride, rinsing the surface with ethanol, and applying a more negative deposition potential. The most important factor that determines N appears to be the pH. This is shown in Fig. 5. In this figure, the influence of V_d can also be seen.

A possible explanation for the different behavior after the various preparations may be as follows: as was seen by Fukidome et al. [28], there is an oxide layer present on the silicon surface after an alkaline fluoride treatment. We believe that this is the case in the experiments of groups 2, 3, and 4, since the substrates in those groups were always hydrophilic after the fluoride treatment. This oxide layer may act as a barrier for electron transfer, which explains the lower currents and hence the lower particle densities after treatments at higher pH. The observed effects of HF and HNO_3 on the particle density may be explained by the thickness of the oxide layer: a high HF concentration will attack the oxide layer more, so it will become thinner. The nitric acid oxides silicon, so at higher concentrations the oxide layer becomes thicker and electron transfer, is more hindered.

In order to verify this explanation, ellipsometric measurements were performed. In these measurements, after the fluoride dip, the substrates (without metal particles) were measured and analyzed for the thickness of the oxide layer. The results in Fig. 6 show that only the pH has a significant influence; as the pH is increased, the layer becomes thicker (the results must be interpreted in a relative manner, rather then in an absolute way. This is due to the small thicknesses (several nanometer)). This was also established with a statistical analysis of the results on the 95% confidence level. An effect of HF and HNO_3 was not observed. This might be because their effect is too small to be observed, due to the low resolution of the method on this scale. The fact that a small oxide layer was seen after a low pH treatment can probably be explained by the practical problem that ellipsometric measurements could not be performed immediately after the treatment (this time interval was 1 h for all experiments).

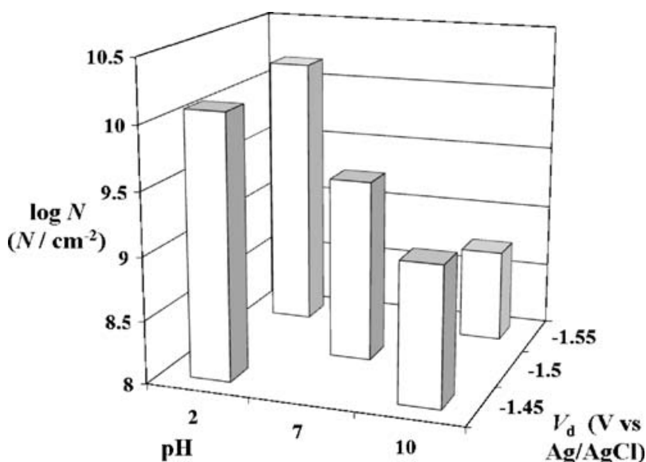

Fig. 5 Logarithm of the particle density obtained with surface analysis as a function of the pH of the fluoride solution and the deposition potential

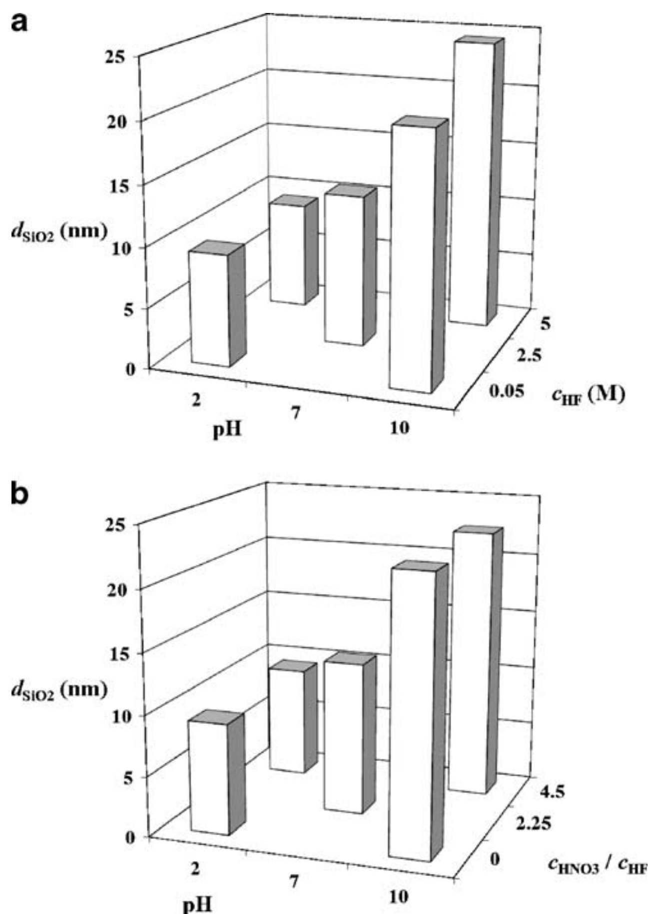

Fig. 6 The thickness of the Si oxide layer as a function of the three factors (pH and c_{HF} in **a**, pH and c_{HNO3}/c_{HF} in **b**) concerning the fluoride treatment of the substrate. Only the pH has a significant influence

The particle size was not analyzed in this stage. For every experiment, the deposition time was held constant at

Table 2 The factors and their levels used in the CCC design

F	L				
	−1	−0.5	0	0.5	1
pH	0	1	2	3	4
c_{HNO3}/c_{HF}	0	0.25	0.5	0.75	1
c_{HF} (M)	1	2	3	4	5
Rinse	Water	Methanol	Ethanol	Propanol	Butanol
V_d (V vs. Ag/AgCl	−1.7	−1.6	−1.5	−1.4	−1.3

F factors, *L* level

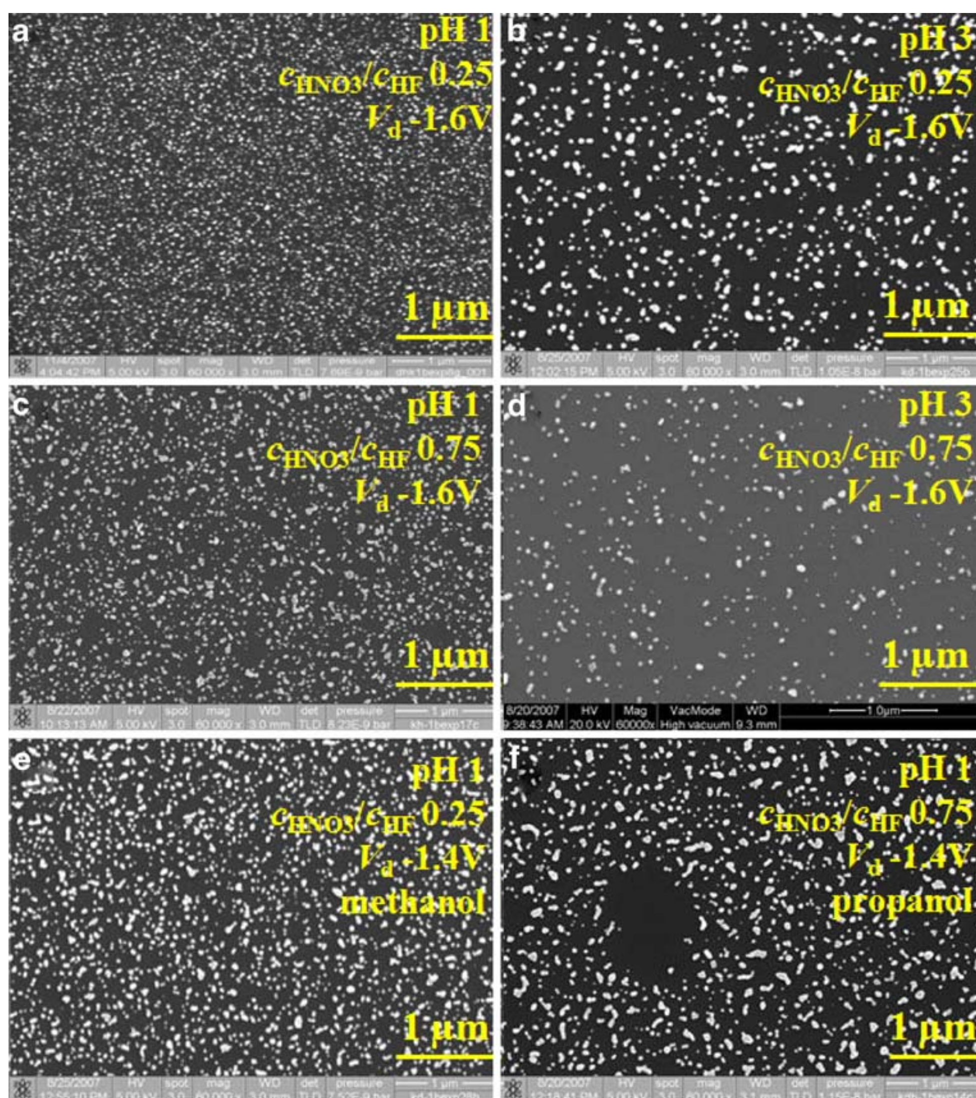

Fig. 7 SEM images of different experiments in the CCC design. The effect of the factors can be seen: the surface is more homogeneous when the pH of the fluoride solution is low (compare **a**–**b** and **c**–**d**), when small amounts of c_{HNO3} are added (compare **a**–**c** and **b**–**d**) and when more negative deposition potentials are applied (compare **a**–**e**)

5 s, so no limit was set for the total charge, hence total amount of gold deposited.

CCC design

In a second series of experiments, the process was studied in more detail, with the ranges of the factors narrowed down according to the results of the first series. From these results, rinsing with ethanol seemed better for a large particle density (see "The 2^{5-1} fractional factorial design approach" section), so the series of rinse solvents was broadened with chain length. Also, more deposition potentials were applied. The factors and their levels are listed in Table 2.

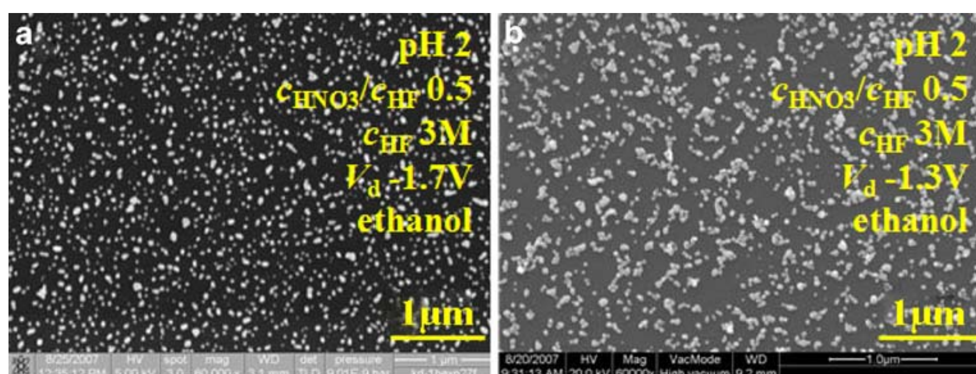

Fig. 8 SEM images of particles deposited at −1.70 V (**a**) and −1.30 V (**b**): more and bigger clusters are formed with less negative deposition potential

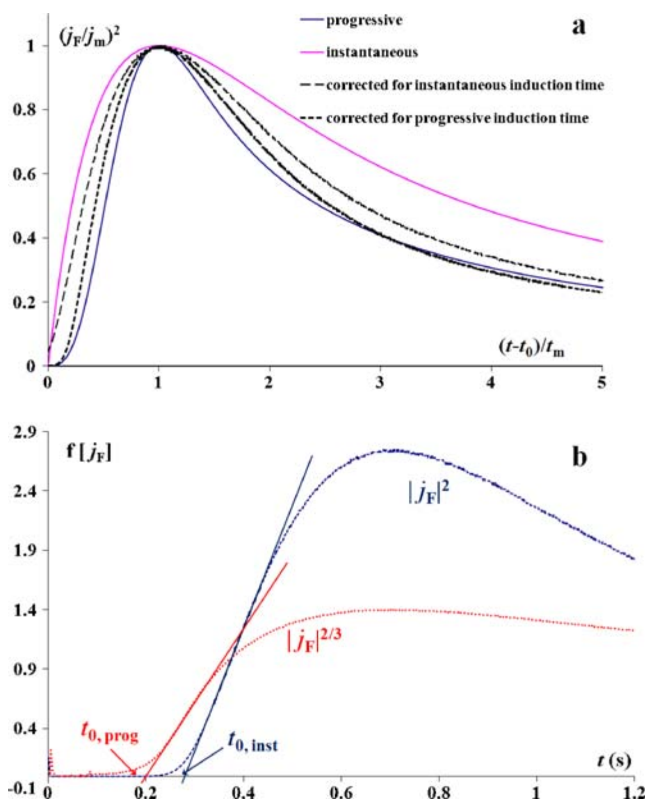

Fig. 9 **a** Dimensionless, corrected transient, recorded at *n*-Si after a surface treatment with 4 M HF+3 M HNO_3 at pH 1 and rinse with propanol at −1.40 V vs. Ag/AgCl in a solution of 1 M KOH+1 M KCN+5 mM $KAu(CN)_2$. Theoretical curves for instantaneous and progressive nucleation are also shown. **b** Linear areas of the $j_F^{2/3}$, respectively, j_F^2 vs. *t* curves, extrapolation allows the determination of the induction time for progressive nucleation $t_{0,prog}$, respectively, instantaneous nucleation $t_{0,inst}$

In this series of experiments, the overall charge of each deposition experiment was limited to a total value of −6 mC. A hydrophobic surface was always observed after the fluoride dip of the silicon. All the results for homogeneity, particle density and particle size distribution were statistically analyzed and following trends were observed.

For homogeneity, an influence was observed of pH, the concentration of nitric acid in the fluoride solution and V_d. Examples of substrates after deposition can be seen in Fig. 7. A more homogeneous surface was seen for the lowest values of pH (Fig. 7a–b and c–d) and a low HNO_3 concentration (Fig. 7a–c and b–d). An effect of the HF concentration was not observed. With a more negative deposition potential, a slightly more homogeneous surface is obtained (Fig. 7a–e). In the "Experimental" section, the homogeneity was defined as the relative standard deviation of the particle density measured on different locations on the same substrate. Another way to define the homogeneity is as the percentage of particles that form clusters. With this definition, the same effect of pH and HNO_3 was observed. Most extreme, however, was the effect of the deposition potential on the clustering: at V_d=−1.3 V, 78% of the particles were clustered (big clusters) while with V_d= −1.7 V only 30% (small clusters). This effect is illustrated in Fig. 8. Some substrates which were rinsed with the higher alcohols had droplet like spots on the surface in which no particles were deposited (Fig. 7f).

For all experiments, the particle densities varied between 2.5 10^9 and 1.5 10^{10} cm^{-2}. The highest coverages were related with the most negative deposition potentials. Also, a lower pH and lower c_{HNO3} promoted higher densities. No significant effect was seen for the hydrogen fluoride concentration and rinse solvent.

For the analysis of particle size distribution, the clustered particles were not considered. The average size varied

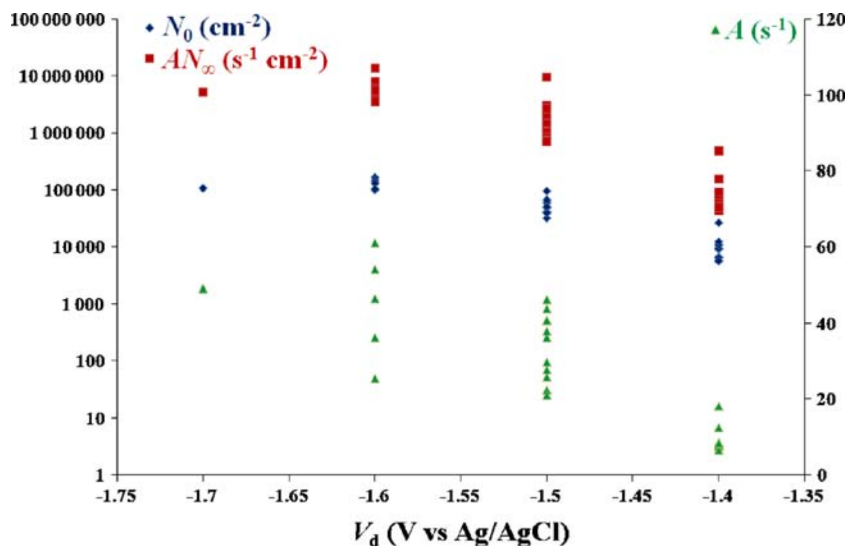

Fig. 10 Values of N_0, AN_∞, and A obtained through transient analysis in the CCC design as a function of the deposition potential V_d

between 18 and 35 nm, depending on the experiment. As a value for the size distribution, the relative standard deviation of the mean size was determined and the values ranged between 0.2 and 0.5. No significant effects were seen, however.

From transient analysis, it followed that each experimental curve showed a mixed progressive/instantaneous nucleation behavior. This is illustrated by a typical example in Fig. 9: Fig. 9a shows the corrected and normalized transients compared to the theoretical curves for instantaneous and progressive nucleation. It can be seen that the experimental curves are in between the theoretical ones. Figure 9b shows that for instantaneous as well as progressive nucleation, induction times t_0 could be determined [21, 22], indicating that during the nucleation process, a period of progressive particle formation proceeds instantaneous nucleation. These findings are in agreement with the results from SEM analysis for particle size distribution.

The global number of active sites N_0 and the nucleation rate constant A were determined under the assumption of pure instantaneous nucleation, while AN_∞ was determined from analysis assuming pure progressive nucleation [19, 20, 22], N_∞ being the maximum number of nuclei that can be formed under circumstances of interfering diffusion fields. The values of N_0, A, and AN_∞ were analyzed according to the model of the CCC design and only a significant effect of the deposition potential V_d was seen: the values of these parameters increase with more negative deposition potential, as illustrated in Fig. 10. These results are also consistent with the results from SEM analysis where higher particle densities were observed with more negative deposition potential.

The observed effects can be explained by the termination present on the surface. After a fluoride treatment with low pH, there are mainly dihydrides present on the surface. When the pH is raised, the number of monohydrides becomes more important. This is a consequence of the reactive species present in the solution. Silicon at the surface can either be initially attacked by small fluoride species or the big OH^- ions [29, 30]. At low pH, the fluoride species is the dominating reactant, which etches the surface in an isotropic fashion. As the hydroxide concentration rises, the reaction with hydroxide becomes more important. Due to sterical hindrance, it is easier for the hydroxide to attack silicon which has two or three hydride bonds, so more monohydrides are left on the surface. As already mentioned in the "Introduction" section, these monohydrides appear in small facets on the surface. This explains the pH dependence of particle density and homogeneity. Monohydride facets are flat and relatively stable, so nucleation is more difficult at these sites compared to the rough di- and trihydride locations. Fewer particles are thus deposited and the surface is covered with small areas in which no particles were deposited. We believe that a possible explanation for the effect of nitric acid is that when there is too much added to the etching solution, small oxide islands are left on surface, which cover the surface locally. When a more negative deposition potential is applied, more nucleation sites are activated which results in more particles and less clusters.

In all the above-discussed results, there was a rather poor fit of the quadratic model with interactions (R^2=0.7/0.8). We believe that the main cause of the error may be due to the effect of the pH of the electrolyte solution used for deposition (an alkaline solution was used for safety reasons): indeed, it is known that OH^- etches silicon, and some of the effects of the fluoride preparation were probably diminished by this reaction.

Conclusions

It was shown that the surface preparation is crucial for the properties of electrodeposited gold on silicon. More homogeneous surfaces and higher particle densities are obtained when the silicon substrate is dipped in a fluoride solution which has a low pH (0–1) and a low ratio of nitric acid to hydrogen fluoride (0–0.25). Electrodeposition at more negative potentials also results in more homogeneity, less and smaller clusters, and higher particle densities. A surface treated with a neutral or alkaline fluoride solution has an oxide layer on top which acts as a barrier for electron transfer. The influence of these results on the growth of Si nanowires will be reported in a following article.

Acknowledgments The authors would like to thank the IWT (Instituut voor Innovatie door Wetenschap en Technologie)—Flanders (SBO project 060031) and Ghent University (BOF project 05B02406) for the financial support. IMEC (Leuven, Belgium) is gratefully acknowledged for the wafer supply and SEM imaging.

References

1. Sivakov V, Andrä G, Himcinschi C, Gösele U, Zahn DRT, Christiansen S (2006) Appl Phys A 85:311–315
2. Hannon JB, Kodambaka S, Ross FM, Tromp RM (2006) Nature Lett 440:69–71
3. Wagner RS, Ellis WC (1964) Appl Phys Lett 4:89–90
4. Meng CY, Shih BL, Lee SC (2007) J Nanopart Res 9:657–660
5. Cui Y, Lauhon LJ, Gudiksen MS, Wang J, Lieber CM (2001) Appl Phys Lett 78:2214–2216
6. Yoon M, Lin XF, Chizhov I, Mai H, Willis RF (2001) Phys Rev B 64:85321–1–85321-5
7. Chen M, Horn RG (2007) J Colloid Interface Sci 315:814–817
8. Kozhevin VM, Yavsin DA, Kouznetsov VM, Busov VM, Mikushkin VM, Nikonov SY, Kolobov A, Gurevich SA (2000) J Vac Sci Technol B 18:1402–1405
9. Oskam G, Long JG, Natarajan A, Searson PC (1998) J Phys D Appl Phys 31:1927–1949

10. Pletcher D (1991) A first course in electrode processes. The Electrochemical Consultancy (Ramsey) Ltd, Hants
11. Munford ML, Maroun F, Cortès R, Allongue P, Pasa AA (2003) Surf Sci 537:95–112
12. Zhang XG (2001) Electrochemistry of Silicon and its Oxide. Kluwer Academic/Plenum, New York
13. Higashi GS, Chabal YJ, Trucks GW, Raghavachari K (1990) Appl Phys Lett 56:656–658
14. Takahagi T, Ishitani A, Kuroda H, Nagasawa Y (1991) J Appl Phys 69:803–807
15. Sunada T, Yasaka T, Takakura M, Sugiyama T, Miyazaki S, Hirose M (1990) Jap J Appl Phys 29:L2408–L2410
16. Robbins HR, Schwartz B (1959) J Electrochem Soc 106:505–508
17. Turner DR (1960) J Electrochem Soc 107:810–816
18. Liu Z, Sun T, An J Wang J (2007) J Electrochem Soc 154:D21–D29
19. Scharifker B, Mostany J (1984) J Electroanal Chem 177:13–23
20. Scharifker B, Hills GJ (1983) Electrochim Acta 28:879–889
21. Gunawardena GA, Hills GJ, Montenegro I (1978) Electrochim Acta 23:693–697
22. Gunawardena GA, Hills GJ, Montenegro I, Scharifker B (1982) J Electroanal Chem 138:225–239
23. Kutner MH, Nachtsheim CJ, Neter J, Li W (2005) Applied linear statistical models, 5th edn. McGraw-Hill, New York
24. Oskam G, Searson PC (2000) Surf Sci 446:103–111
25. Oskam G, Searson PC (2000) J Electrochem Soc 147:2199–2205
26. Vereecken PM, Strubbe K, Gomes WP (1997) J Electroanal Chem 433:19–31
27. Milchev A (2002) Electrocrystallization. Kluwer Academic, Massachusetts
28. Fukidome H, Ohno T, Matsumura M (1997) J Electrochem Soc 144:679–682
29. Hu SM, Kerr DR (1967) J Electrochem Soc 114:414–414
30. Willeke G, Kellermann K (1996) Semicond Sci Technol 11:415–421